Reversible Energy Absorbing Meta-Sandwiches by 4D FDM Printing

M. Bodaghi[1,†], A. Serjouei[1], A. Zolfagharian[2], M. Fotouhi[3], R. Hafizur[1] and D. Durand[1,4]

[1]Department of Engineering, School of Science and Technology, Nottingham Trent University, Nottingham, NG11 8NS, United Kingdom
[2]School of Engineering, Deakin University, Geelong, Victoria 3216, Australia
[3]School of Engineering, University of Glasgow, Glasgow, G12 8QQ, United Kingdom
[4]Département de Génie Mécanique, INSA Toulouse, 31400 Toulouse, France

A B S T R A C T

The aim of this paper is to introduce dual-material auxetic meta-sandwiches by four-dimensional (4D) printing technology for reversible energy absorption applications. The meta-sandwiches are developed based on an understanding of hyper-elastic feature of soft polymers and elasto-plastic behaviors of shape memory polymers and cold programming derived from theory and experiments. Dual-material lattice-based meta-structures with different combinations of soft and hard components are fabricated by 4D printing fused deposition modelling technology. The feasibility and performance of reversible dual-material meta-structures are assessed experimentally and numerically. Computational models for the meta-structures are developed and verified by the experiments. Research trials show that the dual-material auxetic designs are capable of generating a range of non-linear stiffness as per the requirement of energy absorbing applications. It is found that the meta-structures with hyper-elastic and/or elasto-plastic features dissipate energy and exhibit mechanical hysteresis characterized by non-coincident compressive loading-unloading curves. Mechanical hysteresis can be achieved by leveraging elasto-plasticity and snap-through-like mechanical instability through compression. Experiments also reveal that the mechanically induced plastic deformation and dissipation processes are fully reversible by simply heating. The material-structural model, concepts and results provided in this paper are expected to be instrumental towards 4D printing tunable meta-sandwiches for reversible energy absorption applications.

Keywords:

Shape memory polymers; Hyper-elastics; Auxetics; Sandwich; 4D printing; Energy absorption.

[†] Corresponding Author. Tel.: +44-115-84-83470.
E-mail address: mahdi.bodaghi@ntu.ac.uk

1. Introduction

Meta-materials are man-made materials shaped from repeating unit cells that are designed to achieve unique multi-functional properties that cannot be found in nature [1]. These structures gain the extraordinary thermo-mechanical properties from their architecture and programmed structures, rather than the bulk behavior of their elements. Meta-materials exhibit interesting features such as zero/negative Poisson's ratio (auxetic behaviors) [2], variable softening/hardening [3], effective thermal properties [4, 5], and unusual dynamical behaviors [6, 7].

Energy absorbing structures can be found in the nature. Bones, teeth, woods, antlers, teeth, horns and hooves are some examples of natural energy absorbers [8]. Meta-materials and bio-inspired cellular structures are extensively designed for energy absorption applications such as crash mitigation in vehicles and airplanes, protective packaging of sensitive elements and personal/sportive protection equipment. They can experience large compressive strains at almost constant stress level absorbing a large amount of energy without inducing high stress level. The principle of energy absorption in meta-materials and lattice-based structures provides the capability to convert kinetic energy into other types of energies through elastic and/or plastic deformations, mechanical instability and structural collapse [8-10]. Among various energy absorption mechanisms, plastic deformation in ductile materials like metals and polymers has been the most effective classical method to absorb energy [8, 10]. Tan *et al.* [10] proposed stainless steel meta-materials that dissipate energy through instability and plastic deformation. Cyclic loading-unloading compression experiments were conducted to test the structure's repeatability, and annealing treatment was carried out to improve it. The results showed that the structure is repeatable but its repeatability declines as its dimensions increase. The disadvantage of these kinds of energy absorbers is that failure by fracture may occur during loading-unloading and plastic deformation growth. Shape memory alloys such as nickel-

titanium (*NiTi*) have been employed to introduce reversible energy absorbers with shape memory effect and super-elasticity feature [11, 12]. Their energy absorption mechanism is based on the recoverable macroscopic austenitic-martensitic phase transformations. Yuan *et al.* [13] proposed a thermo-mechanically triggered two-stage pattern switching approach, where an amorphous polymer and a flexible elastomer were incorporated in periodic lattices ranging from square mesh, re-entrant honeycomb to tetrachiral lattice.

In recent years, additive manufacturing technologies, well-known as three-dimensional (3D) printing, have enabled fabrication of meta-materials and lattice-based structures for elastic and elasto-plastic deformations [14]. For instance, Bates *et al.* [15] studied energy absorption capacity of hyper-elastic thermoplastic polyurethanes honeycombs fabricated by fused deposition modeling (FDM). The honeycomb density was graded by varying cell wall thickness through the structures to absorb a wide range of compression energies. Habib *et al.* [16] studied in-plane static compressive crushing behavior and energy absorption capacity of polymeric Nylon 12 honeycomb structures of different unit cell thicknesses fabricated by FDM. It was observed that the plastic deformation of hexagonal honeycombs is different in their two main in-plane directions. Taheri Andani *et al.* [17] fabricated *NiTi* shape memory alloys in dense and designed porous forms by selective laser melting (SLM). 3D printed *NiTi* showed good shape memory properties promising for lightweight structures and energy absorbers. Mirzaali *et al.* [18] used 3D printing based on the PolyJet technology to rationally design and fabricate multi-material cellular solids for which the elastic modulus and Poisson's ratio could be independently tailored in different directions. Yazdani Sarvestani *et al.* [19] investigated energy absorption and structural performance of lightweight sandwich polylactic acid (PLA) panels with architected cellular cores of various six-sided cells fabricated by FDM 3D printing. The results showed that the auxetic sandwich panel is an appropriate candidate for energy absorption applications. Al-Saedi *et al.* [20] investigated mechanical properties and energy

absorption capability of functionally graded and uniform F2BCC lattice structures made of Al-12Si Aluminum alloy and manufactured by SLM process. Hedayati *et al.* [21] conducted analytical, numerical and experimental studies to investigate the elastic modulus and yield strength of PLA meta-materials based on the diamond- and cube-shaped unit cells with variable cross sections fabricated by FDM technology. Yang *et al.* [22] improved energy absorption properties of self-locked systems by designing the shape and geometry of tubes made of 3D printed soft-photopolymer resin and hard materials like stainless steel. Alomarah *et al.* [23] investigated compressive properties of polyamide12 auxetic structures 3D printed by Multi Jet Fusion (MJF) method. Xu *et al.* [24] investigated in-plane uniaxial compressive response and energy absorption capacity of a novel hybrid configuration of auxetic and hexagonal honeycomb cells fabricated with nylon material by Object 350 3D printer. The developed meta-structures exhibited superior Young's modulus, collapse strength and energy absorption than traditional honeycomb structures. Geng *et al.* [25] investigated mechanical response, damage initiation and failure evolution of metallic meta-materials fabricated by SLM 3D printing under quasi-static compression. The results showed that the failure behavior of the reentrant lattice is governed not only by its topology, but also by the geometric defects and surface defects. Using 3D printing based on the PolyJet technology, Zhao *et al.* [26] demonstrated the design and validation of the zigzagged periodic lattice-based metamaterials with thermally tunable deformation modes and the thermally switchable Poisson's ratio. By regulating the deformation mode with ambient temperature, the effective Poisson's ratio of the lattice could be intentionally switched between negative values and positive values. In parallel with the growth of conventional 3D printing technologies, 4D printing has been creeping up in the additive manufacturing field. [27]. The 4th dimension associates to "shape change" that 3D printed objects evolve over the time, directly off the print tray. For instance, Li *et al.* [28] introduced 4D printed biodegradable, remotely controllable and personalized shape memory polymer

(SMP) occlusion devices and exemplified atrial septal defect occluders. By incorporating Fe_3O_4 magnetic particles into the SMP matrix, the deployment of the occluders could be controlled remotely after implantation. Xin *et al.* [29] presented a comprehensive review of the mechanical models of SMPs, SMP composites, SMP nanocomposites and their applications in space-deployable structures and 4D printing techniques. Using 4D printing technology, a few researches [30, 31] have been conducted to introduce reconfigurable mechanical single material meta-structures with impact-mitigation capabilities.

Literature review reveals that most of the previous experimental and numerical studies have been directed to investigate energy absorption of single material 3D/4D printed meta-structures under monotonic compressive loading. This paper aims at developing dual-material (soft-hard) auxetic meta-sandwiches by 4D printing FDM technology for reversible energy absorption applications. The conceptual design is based on arranging soft hyper-elastic polymers and elasto-plastic hard SMPs along with cold programming. Dual-material auxetics with different combinations of soft and hard components are 4D printed by FDM technology. It is revealed that the 4D printed meta-structures have great potentials in dissipating kinetic energy due to mechanical hysteresis by leveraging snap-through-like instability and elasto-plasticity. Numerical simulations implementing ANSYS finite element method (FEM) are performed to predict experimental observations on mechanical loading and unloading process. It is found that the non-linear compressive hardening-softening behavior, plateau stress and energy absorption capacity of meta-structures can be replicated accurately by the simulations. The material-structural model, concepts and results provided in this paper are expected to open an avenue for the design and implementation of reversible energy dissipation devices by harnessing shape memory effect (SME), elasto-plasticity, and mechanical instability.

2. Conceptual Design

2.1. Cold programming

SMPs are a class of multi-functional smart materials that can recover shapes after being temporarily deformed via a cold/hot programming protocol. It depends on the temperature zone in which the programming is conducted. In this research, the SMP-based energy absorbers experience a cold-programming-like process during their service in the room temperature that is lower than their glassy transition temperature, T_g. A schematic of the cold-programming protocol for dual SME is illustrated in Fig. 1 in which σ, ε and T signify stress, strain and temperature, respectively. The SMP material, initially in a stress-free glassy state at a temperature lower than its glassy transition temperature ($T = T_l < T_g$), is first deformed mechanically. As can be seen in Fig. 1b, the mechanically applied load must be large enough to induce a plastic strain, ε_p, into the SMP. The process follows as the SMP is unloaded to a temporary deformed shape due to residual plastic deformation, see Fig. 1a and 1b. The material is then heated above the transition temperature range ($T = T_h > T_g$) to recover its original shape known as free strain recovery. As it can be seen, the plastic strain is fully recoverable. The SMP, stable at rubbery phase, is finally cooled down to a low temperature, see Fig. 1. The dissipated energy through the plastic deformation of SMPs, revealed as a hysteresis loop, is considered as the energy absorption mechanism in this work. The SME is also considered to introduce recoverable energy absorbers.

2.2. FDM 3D printing

The process used to fabricate the dual-material lattice-based energy absorbers is FDM which is a filament-based 3D printing technology that follows protocols via computer-aided design (CAD) model and creates physical objects through a layer-by-layer deposition. Before

3D printing the object, the design is created by Autodesk Fusion 360 CAD software then converted to .STL file formats to import into the FDM 3D printer. The dual 3D printer used for this investigation is the 3DGence Double P255 which provides enhanced quality printouts with the features provided. This 3D printer accepts filaments with a diameter of 1.75 *mm* and has features of dual interchangeable hotends which allow dual-material printing of lattice-based structures. It uses a quick change hotend system with patented push system and extrusion quality measurement system that can monitor the quality of each lattice structure. A specialized 3DGence slicing software is implemented which allows adjusting of the .STL print settings. In all 3D printing, unless otherwise stated, the printing speed, layer height and infill density are set 5 *mm/s*, 0.2 *mm*, and 100%, respectively. The raster angle is fixed to be 0^o meaning that all structures are filled in such a way that the printing raster is along the length direction. After the slicer set up is complete, the .STL model is converted into G-code format that allows the 3D-printer to command and control the procedure parameters.

2.3. Material behaviors

The energy absorbers are assumed to be 3D printed with soft and hard components with hyper-elastic and elasto-plastic shape recovery features. FlexPro filaments (RS PRO, Corby, UK) are considered as soft elastomers while polyurethane-based SMP filaments with the glass transition temperature of 60 $°C$ (SMP Technologies Inc., Tokyo, Japan) are selected as hard materials.

Thermo-mechanical properties of the SMPs are characterized using a dynamic-mechanical analyzer (DMA, NETZSCH, Model 242). Beam-like specimens are 3D printed with dimensions of $15mm \times 1mm \times 1.6mm$. The temperature of the nozzle and the build platform is set 195 and 50 ^oC, respectively. DMA tests are performed in an axial mode with forcing frequency of $1Hz$ and heating rate of 5 $°C/min$ varying from -20 to 80 $°C$. The ratio of applied

dynamic stress to static stress is set 1.5. In this paper, for each material/structure three samples are tested to provide clarity of accuracy for the results; and for each series of experiments the arithmetic mean of all values is reported as an average value. In this regard, the results of all the specimens are taken into account due to a good agreement. DMA results in terms of storage modulus, E_s, and $tan(\delta)$ are illustrated in Fig. 2. The storage modulus in the glassy and rubbery phases, at 20 and 80 $^{\circ}C$, is read 1.656 GPa and 3.18 MPa, respectively. It is seen that the SMP phase transformation reduces the storage modulus drastically 520 times. Considering the Young's modulus definition as $E = E_s\sqrt{1 + (tan(\delta))^2}$, it is calculated as $E_g = 1.657\ GPa$ and $E_r = 3.26\ MPa$ for the glassy and rubbery phases, respectively. It is also seen that $tan(\delta)$ graph peaks at $T_g = 60\ ^{\circ}C$ that is considered as the glass transition temperature.

To obtain mechanical properties of the soft and hard materials, dog-bone specimens are 3D printed via FDM based on the dimensions and geometry of ASTM D638 (Type IV, 2 *mm* thickness) [32]. As recommended by the manufacturer, the nozzle temperature for soft and hard materials and the build platform temperature are set 225, 195 and 50 ^{o}C, respectively.

Uniaxial tensile tests are carried out on dog-bone specimens using the Shimadzu® AGS-X 50 *kN* (Kyoto, Kyoto Prefecture, Japan). The Shimadzu® universal machine is equipped with a 1 *kN* load-cell and materials are tested at room temperature ~ 23 $^{\circ}C$ with the speed of 1 *mm/min*. The Trapezium X software is also used as a visual wizard that provides guidance for setting control parameters such as test speed, load capacity and gauge sensors. The gauge marks on dog-bone samples are monitored and tracked to measure the strain of the specimens via advanced non-contact digital video extensometer TRViewX supplied by Shimadzu® and integrated with the Trapezium X. The initial length, L_0, is set 20 *mm*. It should be mentioned that all the tests are conducted in a quasi-static manner (speed =1 *mm/min*) and the strain rate is very low (0.083% s^{-1}) to have no viscosity dependency [33].

The uniaxial tensile results in terms of stress-strain for all specimens are considered due to an acceptable consistency. The experimental stress-strain responses for FlexPro and SMP are illustrated in Fig. 3. F and ΔL indicate force and displacement while A_0 and L_0 stand for original cross-sectional area and length, respectively. FlexPro dog-bones are tested up to 50% strain and all three samples displayed similar graphs with Young's modulus of 66.6 MPa considering initial linear elastic behavior, see Fig. 3a. Although 50% strain is moderately large, the soft FlexPro behaves in a non-linear elastic manner and experiences no residual strain showing qualities of a rubber-like material. Therefore, FlexPro is categorized as a hyper-elastic material. Poisson's ratio is also measured as 0.42. The results presented in Fig. 3a show that SMP reaches maximum stress of 25 MPa before hardening and plasticity starts at 1.4% strain. Young's modulus is calculated as 1.64 GPa from the linear elastic proportion. This is consistent with the Young's modulus obtained from the DMA test as $E_g = 1.657\ GPa$. Poisson's ratio of the SMP is also measured as 0.36. Fig. 3b reveals that the SMP experiences a nearly flat plateau during plastic deformation growth. As the strain rate is very low, the material behavior can be considered as elasto-plastic. Once the applied mechanical load is released gradually, the SMP unloads in a linear elastic manner. It is seen that a residual plastic strain of 27% remains in the dog-bone SMP when it is fully unloaded. The reversibility of this plastic strain is checked by simply heating the sample to the temperature of 85 $°C$, above glass temperature, as shown in Fig. 3b by a red dash-dotted line. As it can be seen, the plastic strain induced by the cold programming process can fully be recovered by heating.

2.4. Auxetic meta-sandwiches

Geometrical parameters of meta-structures play crucial role on the structural performance. Several comprehensive research works [23, 34-39] were conducted on

investigating the effects of geometrical parameters on auxeticity (negative Poisson's ratio) and energy absorption of meta-structures. Yang *et al.* [37] observed that the negative Poisson's ratio increases with increasing re-entrant angle and decreasing horizontal to oblique length ratio. It was shown that for meta-structures made of slender struts (thickness to length ratio is small) the maximum auxeticity occurs at re-entrant angle around 70°-75° and horizontal to oblique length ratio of 2 [37-39]. Regarding the struts thickness, Wang et al. [39] showed that with increase in strut thickness of the re-entrant structure, the auxeticity decreases gradually and finally reaches a plateau while the compression Young's modulus and relative density increase monotonically. It was also proved that the higher the relative density, the larger the energy absorption capacity [34-35]. Hence, increase in strut thickness of the re-entrant auxetic structure results in increase in relative density and therefore increase in energy absorption capacity. The main goal of the present work is to introduce meta-sandwiches with high auxeticity and energy absorption capacity. By considering the fact that the minimum applicable resolution of the FDM 3D printer is 1 *mm*, the re-entrant angle of 70°, horizontal to oblique length ratio of ~2 (overall width of the unit cell is 20 *mm*), and strut thickness of 1 *mm* are assumed as shown in Fig. 4a. They are found to be optimal preventing the internal vertices of the cells in the lattice to contact each other during compression tests. Based on the periodicity concept, the auxetic unit cell is arranged in the plane to form a periodic arrangement as shown in Fig. 4b. The auxetic dual-material energy absorbers are created in CAD format using Autodesk Fusion 360 software. The bottom face of the meta-structure is assumed to be thicker (2 *mm*) that allows the structure to be stable on the compression test platform. It is also 3D printed with 100% infill to make the computational simulation more accurate and prevent the change of results due to a weak internal structure.

Four auxetic structures are created in the following form: pure SMP, pure FlexPro, SMP-FlexPro and FlexPro-SMP. Schematic of SMP-FlexPro and FlexPro-SMP are illustrated

in Fig. 5 where SMP and FlexPro are dominant in these two combinations. The energy absorbing capability of the proposed auxetics is investigated in this research. The indenter used for compression tests is a combination of a semi-circle with a rectangle and extruded on Autodesk Fusion 360 and assumed as a rigid body with a high Young's modulus. It is fabricated by a Formlabs Form 2 desktop stereo-lithography 3D printer (Formlabs Inc., Somerville, USA) from Grey Pro Resin. Its Young's modulus and Poisson's ratio are measured as 2.6 *GPa* and 0.4, respectively.

3. Finite Element Modeling

This section is dedicated to implement a commercial FEM software package as a straightforward tool to accurately simulate mechanical loading-unloading responses of SMP and FlexPro materials. The FEM is established by means of geometrically non-linear software package of ANSYS® workbench to simulate mechanical behaviors of soft-hard dual-meta-sandwiches with hyper-elastic and elasto-plastic features.

The Mooney-Rivlin model is implemented to describe hyper-elastic behaviors of FlexPro materials. Assuming incompressibility and isotropy, the strain energy function, *W*, can be written as:

$$W = c_{10}(\bar{I}_1 - 3) + c_{01}(\bar{I}_2 - 3) \quad (1)$$

where c_{10} and c_{01} are material constants while $\bar{I}_1$ and $\bar{I}_2$ are the first and second invariant of the right Cauchy-Green deformation tensor.

The SMP is assumed to behave as an elasto-plastic material with linear isotropic hardening. The von Mises yield criterion is adapted as:

$$F = \sqrt{\frac{3}{2}}\|\bar{\boldsymbol{\sigma}}\| - \left(\sqrt{\frac{2}{3}}H_p\|\boldsymbol{\epsilon}_p\| + \sigma_y\right) \quad (2)$$

where $\|\ \|$ is the usual Euclidean norm; $\bar{\boldsymbol{\sigma}}$ denotes the deviatoric part of the second order stress tensor, while $\boldsymbol{\epsilon_p}$ is the plastic strain tensor. Also, H_p is a material parameter that controls the hardening during plastic deformation whereas σ_y is a constant yield stress.

Hyper-elasticity and elasto-plasticity are integrated into the geometrically non-linear FEM to trace non-linear equilibrium path via augmented Lagrange and pure penalty formulations. The FEM implemented by ANSYS is expected to serve as a straightforward tool for simulating mechanical loading-unloading cycles. However, it should be mentioned that modeling heating-cooling process in SMPs needs implementing complex constitutive equations [29, 30] that is beyond the aim of the paper and could be considered in future development efforts.

4. Results and Discussions

In this section, the energy absorbing capabilities of 4D printed auxetic meta-sandwiches are demonstrated experimentally and numerically. First, material properties introduced in the modeling section need to be specified. The parameters related to the hyper-elastic and elasto-plastic models including c_{10} and c_{01} in Eq. (1) and σ_y and H_p in Eq. (2) are calibrated using experimental tensile results displayed in Fig. 3. They are selected as 9.6, -3.8, 24.4 and 0.4 *MPa*, respectively, to match stress-strain curves as demonstrated in Fig. 3. This comparison study reveals that the FEM ANSYS predicts well experimental features such as mechanical loading-unloading path, nearly flat plateau during plastic deformation, and non-linear elasticity. It is also concluded that the hyper-elastic and elasto-plastic models are accurate

enough to replicate experiments conducted on FelxPro and SMPs in a quasi-static manner and under the low strain rate of 0.083% s^{-1}.

Next, mechanical behaviors of 4D printed auxetic energy absorbers with different material combinations are studied. The 3D printed indenter is connected to the top of the Shimadzu® compression plate. Each sample is placed on the fixed bottom plate of the testing machine and a displacement-controlled quasi-static mechanical loading is applied to the auxetic structures with the crosshead moving downward at a constant speed of 1 *mm/min*. As the strain rate is very low (0.03% s^{-1}) [33], FlexPro and SMP are expected to exhibit hyper-elastic and elasto-plastic behaviors, respectively. Mechanical responses of all four meta-structures tested at room temperature ~ 23 °*C* in terms of force and central displacement are presented in Fig. 6. The stroke applied on the SMP auxetic meta-structure in the compression test is 20 *mm*. Fig. 6 shows that the SMP meta-structure reaches a maximum force of 144 *N* and after removing the indenter a central displacement of 14.5 *mm* remains via permanent plastic deformation inducing hysteresis and dissipating energy. Since for both dual-material meta-structures, 20 *mm* stroke does not deform the lattices plastically, the stroke of 30 *mm* is applied which deforms the lattices plastically, see Fig. 6. The pure FlexPro meta-structure is also compressed by 30 *mm* stroke showing a hyper-elastic behavior. Fig. 6 shows that hyper-elastic FlexPro meta-structure reaches a maximum force of 13 *N* at stroke 30 *mm* and after unloading the auxetic meta-structure fully recovers all the deformation. It is found that the hyper-elastic FlexPro meta-structure dissipates energy and exhibits hysteresis undergoing a loading-unloading cycle. The overall dissipated energy observed in the experiment can be attributed slightly to visco-elasticity and mainly to mechanical instability through compression. SMP-FlexPro meta-sandwich exceeds the pure SMP meta-structure reaching to 176 *N* with a permanent plastic displacement of 6.9 *mm* after unloading. FlexPro-SMP meta-sandwich reaches a maximum force of 31 *N* and a permanent plastic displacement after unloading of 4.2 *mm*. As it can be

seen, both SMP-FlexPro and FlexPro-SMP meta-sandwiches exhibit hysteresis. The energy dissipation may arise from mechanical instability, plasticity and minor visco-elasticity. As shown in Fig. 6, different patterns of material arrangements can demonstrate different mechanical behaviors. This could also be partially due to the layer of the material the indenter would first contact that changes the mechanical response. Finally, Fig. 6 proves that the proposed meta-structures have great potentials to be used as energy absorbers for different applications.

The non-linear structural FEM tool is then implemented to replicate mechanical responses of 3D printed auxetics. Tet10 and Hex20 elements are selected in ANSYS for the main body and bottom support, respectively. The FEM mesh is generated on the auxetic structures as shown in Fig. 7. The transition is set to slow to increase the simulation precision and the span angle center type is fine elements with mesh defeaturing turned on. The defeaturing accounts for tolerance which defeatures small and dirty geometry that would affect the simulation. Overall statistics of mesh elements and nodes after convergence are 11377 and 26671, respectively. A fully-bonded interface is assumed between soft and hard material elements. The auxetic structures are compressed between the top indenter and the bottom rigid plate. To consider the auxetic unit cells interaction with themselves and the top and bottom rigid bodies during the compression, a surface to surface contact is defined. Furthermore, all degrees of freedom of the bottom plate is fixed while the meta-structure is free to move without any constraints as it is in experiments and the top indenter is allowed to move only in the vertical direction as depicted in Fig. 7.

Experimental and numerical behaviors of four different meta-structures under loading-unloading process at room temperature, 23 $^{\circ}C$, are displayed in Figs. 8-11, respectively, for SMP, SMP-FlexPro, FlexPro-SMP and FlexPro meta-structures. SMP, SMP-FlexPro and FlexPro-SMP meta-structures are also heated to 85 $^{\circ}C$ that is above the transition temperature

range ($T > T_g$) to check shape recovery capability of the energy absorbers. In Figs. 8, 10 and 11, parts (a)-(c) and (e)-(g) display configurations of the meta-structures under loading-unloading obtained from experiments and numerical FEM modeling, respectively, while part (d) depicts the configuration after heating to 85 $°C$ followed by cooling down to the room temperature, 23 $°C$. Part (h) also compares force-displacement curves from experiments and numerical FEM. The dissipated energy and stored energy through mechanical instabilities and plastic deformations are also demonstrated in part (i) of Figs. 8, 10 and 11. The counterpart of Fig. 8 is also illustrated in Fig. 9 for the FlexPro meta-structure with fully hyper-elastic behavior and without any need for shape recovery via heating. It should be mentioned that a white FlexPro material is 3D printed, as shown in Fig. 9, that is contrary to the black background.

The preliminary conclusion drawn from Figs. 8-11 is the fact that FEM implemented by ANSYS as a straightforward tool with material setting calibrated via simple tensile tests can successfully replicate configuration and force-displacement behaviors of different meta-structures with an acceptable accuracy. It is found that the hyper-elastic and elasto-plastic models are accurate enough to simulate meta-structures tested in a quasi-static manner and under the low strain rate of 0.03% s^{-1}. The fully-bonded interface assumed between soft and hard material elements seems also accurate enough for predicating the experimental observations even under large strains with the low rate. Fig. 8 reveals that by applying a compressive mechanical load to the SMP meta-structure, the beam-like members are deformed and experienced local bending and buckling. The meta-structure shows an initial hardening as the force has an increasing trend against the vertical displacement. This is due to the auxetic effect of the structure in the elastic deformation range. A transient behavior of hardening to softening is observed in the range of 2-5 *mm*. After 5 *mm* stroke, the meta-structure seems to lose its stability and experiences a softening snap-through type of buckling, see Fig. 8h. The

force induced in the SMP meta-structure shows a decreasing trend and becomes minimum at stoke of 7.5 *mm*. As can be seen in Fig. 8f, the auxetic structure shrinks in both vertical and horizontal directions by vertical mechanical loading. In fact, when the external indenter further compresses the meta-structure in the vertical direction, the auxetic structure contracts laterally as well and the material flows into the collision location producing a denser structure with a higher collision resistance. This feature affects force-displacement trend and a local hardening behavior (local densification) can be seen in Fig. 8h. The force curves measured from the experiment and FEM solution peak at 130 and 145 *kN*, respectively. After that, a general softening behavior can be seen due to the overall collapse of the auxetic structure. Fig. 8b, 8f and 8h reveal that the meta-structure tends to harden at the end of mechanical loading when the beam members contact each other. The end of the overall plateau regime can be identified by the start of final densification regime when the stress increases, see Fig. 8h. By mechanical unloading, mechanical hysteresis, characterized by noncoincident loading-unloading curves, is observed. The meta-structure recovers its original shape partially while some strains remain in the auxetics indicating the energy dissipation due to the plastic deformation. As a result, the input energy due to the external force is transformed into the kinetic energy and some of it is dissipated via the plastic deformation mechanism. Fig. 8c, 8g and 8h shows that FEM ANSYS can accurately predict the experimental residual plastic deformation in the SMP meta-structure. When the deformed auxetic material is heated, it releases all the plastic strains via solid-state phase transformation and fully recovers its initial shape. It implies that the proposed meta-structure has excellent potential to be used as 4D printed recoverable/reversible energy absorbers. Comparing experimental and numerical results in Fig. 8h reveals that there are small differences in the measured force once the stroke of 10 *mm* is exceeded. This could be due to geometric imperfection in the real lattice structure fabricated by 3D printing, while FEM ANSYS simulation assumes a perfect model with no inconsistencies along its internal beams.

It is seen that FEM simulation results are consistent with the experimental results, and yield stress, plastic deformation growth, unloading path and hysteresis area can accurately be predicted by the simulation. Therefore, the FEM analysis can provide accurate guidance for designing 4D printed recoverable energy absorbers. Next, the energy distribution for SMP meta-structure characterized by the area under the load-displacement curve as shown in Fig. 8i is discussed. The energy dissipation and absorption calculated are 1.95 *J* and 0.3 *J*, respectively, and as expected more energy is dissipated than absorbed for this lattice due to presence of plastic hardening behavior of the SMP with only 13.3% of the total energy absorbed. The SMP lattice would be capable to convert the kinetic energy into other forms via fracture surfaces along the auxetic unit cell members and during plastic deformation under compression.

Mechanical response of FlexPro auxetic lattice is illustrated in Fig. 9 where the hyper-elastic property of the material is observed due to the structure retaining back to its original shape after the end of unloading process which requires no shape recovery procedure. A softening-hardening behavior is observed in Fig. 9g during mechanical loading step. The softening feature can be associated with the overall snap-though buckling of the lattice while it hardens due to the auxetic feature, densification and contact happened between beam-like members producing a denser structure, see Fig. 9b and 9e. Removing the load produces a hysteresis loop between the loading and unloading curves as illustrated in Fig. 9g. It is seen that this hysteresis loop is fully recoverable as the mechanical load is completely removed. As simulation here adopts the Mooney-Rivlin hyper-elastic model, overall dissipation energy mechanism is due to mechanical snap-though-like instability. Focusing on the results presented in Fig. 9g reveals that the experimental hysteresis loop area is a little bit larger than that predicted by FEM because the overall dissipated energy in experiment includes the slight part due to the visco-elasticity plus the main part due to the mechanical instability through compression. It is concluded that the hyper-elastic Mooney-Rivlin model is able to predict key

non-linear characteristics observed during experimentation as shown in Fig. 9a-9c and 9d-9f. As can also be seen in Fig. 9g, there is a strong correlation between experimental and numerical force-stroke curves, and both reach similar maximum forces which are 13.1 *N* and 12.9 *N*, respectively. The FlexPro meta-structure shows opposite trends in energy distributions than that of SMP meta-structure because of the dominant hyper-elastic properties, see Fig. 9h. The total energy distributed is calculated as 0.2175 *J* with 0.0875 *J* accounting for dissipation and 0.13 *J* for absorption. Although the FlexPro lattice is compressed at a higher stroke, it experiences less energy distribution than that of SMP as the soft auxetic unit cells experience much less force during the experiment. It is also found that recoverable FlexPro meta-structure is able to dissipate 40.2% of the total energy by leveraging mechanical instability through compression.

The counterpart of Fig. 8 for SMP-FlexPro and FlexPro-SMP meta-sandwiches is demonstrated in Figs. 10 and 11. As it can be seen, the dual-material meta-sandwich displays a unique deformation behavior compared to that of the single-material lattice counterparts while under vertical compression. Fig. 10 shows that the SMP-FlexPro meta-sandwich initially has a low stiffness despite the hard layer being the first point of contact with the indenter. As can be seen in Fig. 10h, the FlexPro and SMP elements experience respectively maximum and minimum deformation and distortion in the range of 0-13.5 *mm* stroke and the meta-sandwich shows an overall softening behavior with a nearly flat plateau. That is because the kinetic energy from the indenter gradually transfers to soft and hard layers and soft elements with lower stiffness deform more. The meta-sandwich starts to harden from stroke 13.5 *mm* onwards where FlexPro elements have already been deformed and the applied force mostly transfers to hard SMP elements and densification initiates. The coupled effects of the auxetic feature, densification, and plastic deformation of the SMP elements lead overall hardening up to the end of mechanical loading. Upon unloading of the meta-sandwich, it is seen that the induced

force drops drastically and then the structure experiences a nearly flat backward plateau with a low level of the force. This sudden drop occurred in the force-displacement curve is directly related to the irrecoverable plastic deformation remained in the SMP elements and mechanical instability. This leads to a wide hysteresis loop as shown in Fig. 10h. The large and small deformations in FlexPro and SMP elements are recovered, respectively, while a small plastic deformation remains in the auxetic structure at the end of unloading step, see Fig. 10c and 10g. Comparing the residual deformation in SMP and SMP-FlexPro meta-structures reveals that this residual plastic deformation is much less than that of the pure FlexPro lattice. It is worth mentioning that the hyper-elastic FlexPro beams show some deformations that is because they are locked by SMP beam-like members with residual plastic deformations. Fig. 10d also reveals that heating the auxetic fully releases the residual plastic deformation. The FEM simulation shows a close estimation of the non-linear mechanical behavior, hysteresis loop, residual plastic deformation, densification and configuration observed in the experiment. Regarding energy distribution from the quantitative point of view, it is worthwhile to mention that energy absorption/dissipation of SMP-FlexPro lattice is located between those of the pure SMP and FlexPro meta-structures. Fig. 10i shows the energy distribution with energy dissipation represented by the hysteresis loop. The total energy is calculated as 1.725 *J* with energy dissipation of 1.3 *J* and energy absorption of 0.425 *J*. Compared to the SMP lattice, SMP-FlexPro dissipates less energy while absorbs more energy allowing the structure to recover a larger part of deformation.

Fig. 11h shows that the FlexPro-SMP lattice has a trend of hardening followed by softening and then hardening. The coupled influences of the auxetic property, snap-though-like instability, densification, and SMP plastic deformation lead this mechanical behavior. In both experimental and numerical studies, the lattice experiences a hardening-softening-like behavior from 0 to 13 *mm* stroke followed by a softening-hardening from approximately 14 *mm* to 23

mm stroke. An overall good agreement between experimental observation and FEM results is detected on this pattern. However, approximately between stroke 26.5 *mm* to 30 *mm* there is a subtle difference where the experiment displays softening-hardening and FEM simulation continues to harden. This could be due to the presence of some very small defects in the lattice along the layers formed during FDM 3D printing that may cause inaccuracies like this extra softening when highly compressed. The maximum force from the FEM solution is 31.5 *N* which matches 31 *N* from the experiment. Once the mechanical loading is removed, the lattice deformation is partially recovered while a small residual deformation remains in the meta-sandwich at the end of loading stage due to the plastic strains in SMP members, see Fig. 11c and 11g. Since the FlexPro-SMP meta-structure has more FlexPro members compared to the SMP-FlexPro one, removing the load from the lattice produces a more gradual unloading graph. As it also can be observed, FlexPro members in the top and middle of the meta-sandwich experience some deformation due to the plastic deformation in their neighbor SMP links. Again, it is found that the mechanically induced plastic strain is fully recovered by simply heating as shown in Fig. 11d. Dual-material FlexPro-SMP meta-sandwich also reveals energy absorption up to 38% of total energy experienced, see Fig. 11i. The energy statistics follows as 0.2795 *J* for energy dissipation and 0.168 *J* for absorption. It can be found that the energy absorption with respect to total energy for FlexPro-SMP is 14% more than SMP-FlexPro. This is due to the fact that the soft layer of the FlexPro-SMP meta-sandwich is contacted by the indenter first. Moreover, the soft FlexPro layers are more efficient in energy absorption than the SMP layers. Therefore FlexPro-SMP shows a higher energy absorption as the stress towards the core of the auxetic sandwich is minimized.

5. Conclusion

The present research was dedicated to exploring reversible energy absorbing meta-sandwiches manufactured by 4D FDM printing technology. The concept was on the basis of arranging soft hyper-elastic polymers with elasto-plastic SMPs to engineer dual-material auxetic structures. 4D FDM printing was implemented to fabricate sandwich auxetics with different combinations of soft and hard components. FEM models were developed using ANSYS to accurately simulate the behaviors of the 4D printed meta-structures under a compressive loading-unloading cycle. The feasibility and performance of the tunable reversible meta-structures were assessed experimentally and numerically. It was found that dual-material auxetic designs are capable of generating a range of non-linear stiffness and dissipating energy as per the requirement of energy absorbing applications. The underlying mechanism for the existence of hysteresis loop, the physics of snap-through instability, and elasto-plasticity was unveiled. Comparison studies revealed that the main aspects of meta-sandwiches were well simulated in capturing yield stress, plateau during plastic deformation growth, unloading path and hysteresis area. It was also experimentally shown that the deformation and the dissipation processes are reversible opening an avenue for the design and implementation of recoverable energy dissipation devices for impact protection and shock mitigation applications. Due to the absence of similar concept and results in the specialized literature, this paper is likely to advance the state-of-the-art 4D printing tunable meta-sandwiches with reversible energy absorption features.

References

[1] Saxena, K.K., Das, R. and Calius, E.P., 2016. Three decades of auxetics research− materials with negative Poisson's ratio: a review. Advanced Engineering Materials, 18(11), pp.1847-1870.

[2] Chen, Y., Li, T., Scarpa, F. and Wang, L., 2017. Lattice metamaterials with mechanically tunable Poisson's ratio for vibration control. Physical Review Applied, 7(2), p.024012.

[3] Bodaghi, M., Damanpack, A.R., Hu, G.F. and Liao, W.H., 2017. Large deformations of soft metamaterials fabricated by 3D printing. Materials & Design, 131, pp.81-91.

[4] Mirabolghasemi, A., Akbarzadeh, A.H., Rodrigue, D. and Therriault, D., 2019. Thermal conductivity of architected cellular metamaterials. Acta Materialia, 174, pp.61-80.

[5] Li, X., Gao, L., Zhou, W., Wang, Y. and Lu, Y., 2019. Novel 2D metamaterials with negative Poisson's ratio and negative thermal expansion. Extreme Mechanics Letters, 30, p.100498.

[6] Nimmagadda, C. and Matlack, K.H., 2019. Thermally tunable band gaps in architected metamaterial structures. Journal of Sound and Vibration, 439, pp.29-42.

[7] Moscatelli, M., Ardito, R., Driemeier, L. and Comi, C., 2019. Band-gap structure in two- and three-dimensional cellular locally resonant materials. Journal of Sound and Vibration, 454, pp.73-84.

[8] Svensson, E., 2017. Material characterization of 3D-printed energy-absorbent polymers inspired by nature. CHALMERS University of Technology.

[9] Sun, S., An, N., Wang, G., Li, M. and Zhou, J., 2019. Snap-back induced hysteresis in an elastic mechanical metamaterial under tension. Applied Physics Letters, 115(9), p.091901.

[10] Tan, X., Chen, S., Zhu, S., Wang, B., Xu, P., Yao, K. and Sun, Y., 2019. Reusable metamaterial via inelastic instability for energy absorption. International Journal of Mechanical Sciences, 155, pp.509-517.

[11] Nemat-Nasser, S., Choi, J.Y., Isaacs, J.B. and Lischer, D.W., 2006. Quasi-static and dynamic buckling of thin cylindrical shape-memory shells. Journal of applied mechanics, 73(5), pp.825-833.

[12] Jiang, D., Bechle, N.J., Landis, C.M. and Kyriakides, S., 2016. Buckling and recovery of NiTi tubes under axial compression. International Journal of Solids and Structures, 80, pp.52-63.

[13] Yuan, C., Mu, X., Dunn, C.K., Haidar, J., Wang, T. and Jerry Qi, H., 2018. Thermomechanically triggered two-stage pattern switching of 2D lattices for adaptive structures. Advanced Functional Materials, 28(18), p.1705727.

[14] Zadpoor, A.A., 2019. Additively manufactured porous metallic biomaterials. Journal of Materials Chemistry B. 7, 4088-4117.

[15] Bates, S.R., Farrow, I.R. and Trask, R.S., 2016. 3D printed polyurethane honeycombs for repeated tailored energy absorption. Materials & Design, 112, pp.172-183.

[16] Habib, F.N., Iovenitti, P., Masood, S.H. and Nikzad, M., 2017. In-plane energy absorption evaluation of 3D printed polymeric honeycombs. Virtual and Physical Prototyping, 12(2), pp.117-131.

[17] Andani, M.T., Saedi, S., Turabi, A.S., Karamooz, M.R., Haberland, C., Karaca, H.E. and Elahinia, M., 2017. Mechanical and shape memory properties of porous $Ni_{50.-1}Ti_{49.9}$ alloys manufactured by selective laser melting. Journal of the mechanical behavior of biomedical materials, 68, pp.224-231.

[18] Mirzaali, M.J., Caracciolo, A., Pahlavani, H., Janbaz, S., Vergani, L. and Zadpoor, A.A., 2018. Multi-material 3D printed mechanical metamaterials: Rational design of elastic properties through spatial distribution of hard and soft phases. Applied Physics Letters, 113(24), p.241903.

[19] Yazdani Sarvestani, H., Akbarzadeh, A.H., Niknam, H. and Hermenean, K., 2018. 3D printed architected polymeric sandwich panels: Energy absorption and structural performance. Composite Structures, 200, pp.886-909.

[20] Al-Saedi, D.S., Masood, S.H., Faizan-Ur-Rab, M., Alomarah, A. and Ponnusamy, P., 2018. Mechanical properties and energy absorption capability of functionally graded F2BCC lattice fabricated by SLM. Materials & Design, 144, pp.32-44.

[21] Hedayati, R., Salami, S.J., Li, Y., Sadighi, M. and Zadpoor, A.A., 2019. Semianalytical Geometry-Property Relationships for Some Generalized Classes of Pentamodelike Additively Manufactured Mechanical Metamaterials. Physical Review Applied, 11(3), p.034057.

[22] Yang, K., Chen, Y., Zhang, L., Xiong, F., Hu, X. and Qiao, C., 2019. Shape and geometry design for self-locked energy absorption systems. International Journal of Mechanical Sciences, 156, pp.312-328.

[23] Alomarah, A., Masood, S.H., Sbarski, I., Faisal, B., Gao, Z. and Ruan, D., 2019. Compressive properties of 3D printed auxetic structures: experimental and numerical studies. Virtual and Physical Prototyping, pp.1-21.

[24] Xu, M., Xu, Z., Zhang, Z., Lei, H., Bai, Y. and Fang, D., 2019. Mechanical properties and energy absorption capability of AuxHex structure under in-plane compression: Theoretical and experimental studies. International Journal of Mechanical Sciences, 159, pp.43-57.

[25] Geng, L., Wu, W., Sun, L. and Fang, D., 2019. Damage characterizations and simulation of selective laser melting fabricated 3D re-entrant lattices based on in-situ CT testing and geometric reconstruction. International Journal of Mechanical Sciences, 157, pp.231-242.

[26] Zhao, Z., Yuan, C., Lei, M., Yang, L., Zhang, Q., Chen, H., Qi, H.J. and Fang, D., 2019. Three-dimensionally printed mechanical metamaterials with thermally Tunable auxetic behavior. Physical Review Applied, 11(4), p.044074.

[27] Ding, H., Zhang, X., Liu, Y. and Ramakrishna, S., 2019. Review of mechanisms and deformation behaviors in 4D printing. The International Journal of Advanced Manufacturing Technology, pp.1-17.

[28] Lin, C., Lv, J., Li, Y., Zhang, F., Li, J., Liu, Y., Liu, L. and Leng, J., 2019. 4D-printed biodegradable and remotely controllable shape memory occlusion devices. Advanced Functional Materials, 1906569.

[29] Xin, X., Liu, L., Liu, Y. and Leng, J., 2019. Mechanical models, structures, and applications of shape-memory polymers and their composites. Acta Mechanica Solida Sinica, 32(5), pp.535-565.

[30] Bodaghi, M. and Liao, W.H., 2019. 4D printed tunable mechanical metamaterials with shape memory operations. Smart Materials and Structures, 28(4), p.045019.

[31] Yang, C., Boorugu, M., Dopp, A., Ren, J., Martin, R., Han, D., Choi, W. and Lee, H., 2019. 4D printing reconfigurable, deployable and mechanically tunable metamaterials. Materials Horizons, 6, 1244-1250.

[32] ASTM International, 2015. ASTM D638-14, Standard Test Method for Tensile Properties of Plastics. ASTM International.

[33] Guo, X., Liu, L., Zhou, B., Liu, Y. and Leng, J., 2015. Influence of strain rates on the mechanical behaviors of shape memory polymer. Smart Materials and Structures, 24(9), p.095009.

[34] Yuan, S., Chua, C. K. and Zhou, K., 2019. 3D-Printed mechanical metamaterials with high energy absorption. Advanced Materials Technologies, 4 (3), 1800419.

[35] Gibson, L. J. and Ashby, M. F., 1997. Cellular solids: Structure and properties; Cambridge University Press.

[36] Li, D., Liao, W., Dai, N. and Xie, Y. M., 2019. Comparison of mechanical properties and energy absorption of sheet-based and strut-based gyroid cellular structures with graded densities. Materials, 12 (13), 2183.

[37] Yang, L., Harrysson, O., West, H. and Cormier, D., 2015. Mechanical properties of 3D re-entrant honeycomb auxetic structures realized via additive manufacturing. International Journal of Solids and Structures, 69-70, 475-490.

[38] Li, S., Hassanin, H., Attallah, M. M., Adkins, N. J. E. and Essa, K., 2016. The development of TiNi-based negative Poisson's ratio structure using selective laser melting. Acta Materialia, 105, 75-83.

[39] Wang, X.T., Li, X.W. and Ma, L., 2016. Interlocking assembled 3D auxetic cellular structures. Materials and Design, 99, 467-476.

List of Figures

(a)

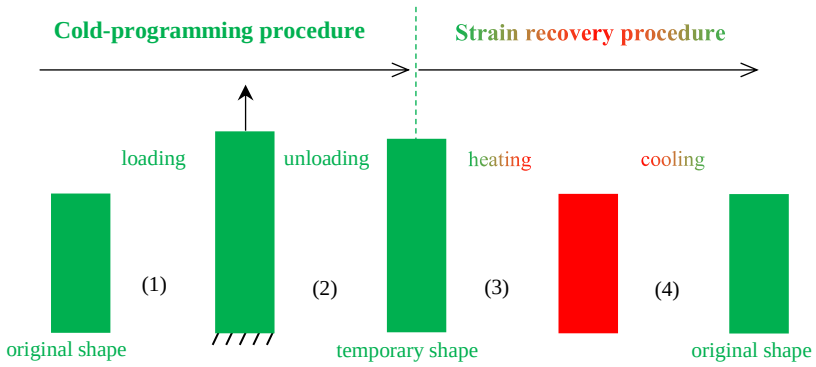

(b)

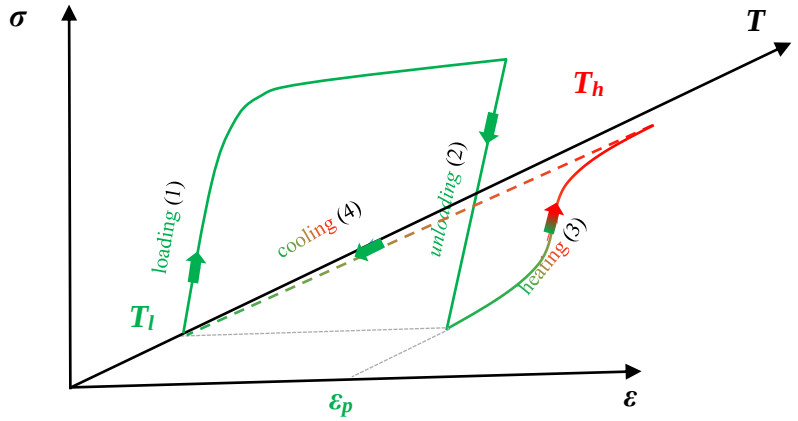

Figure 1. SMP cold programming: (a) thermo-mechanical procedure, (b) stress-strain temperature diagram.

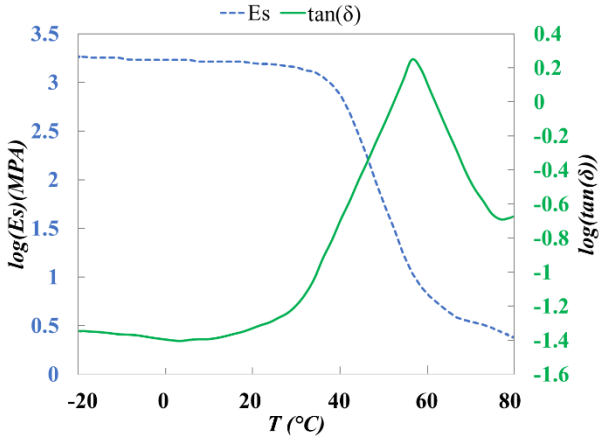

Figure 2. DMA measurement result on the 3D printed SMP in terms of storage modulus (E_s) and *tan (δ)*.

(a)

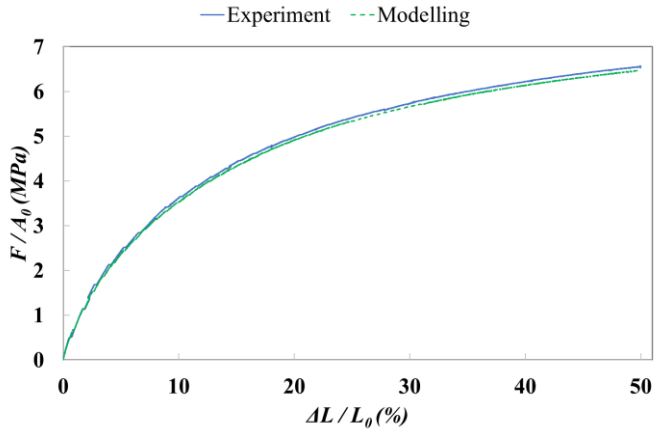

(b)

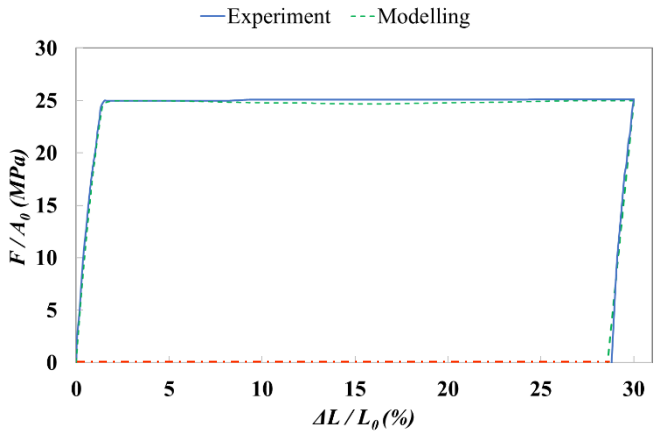

Figure 3. Experimental and numerical uniaxial tensile tests in terms of stress-strain: (a) FlexPro, (b) SMP (experimental free strain recovery by thermal loading is represented by the red dash-dotted line).

(a) **(b)**

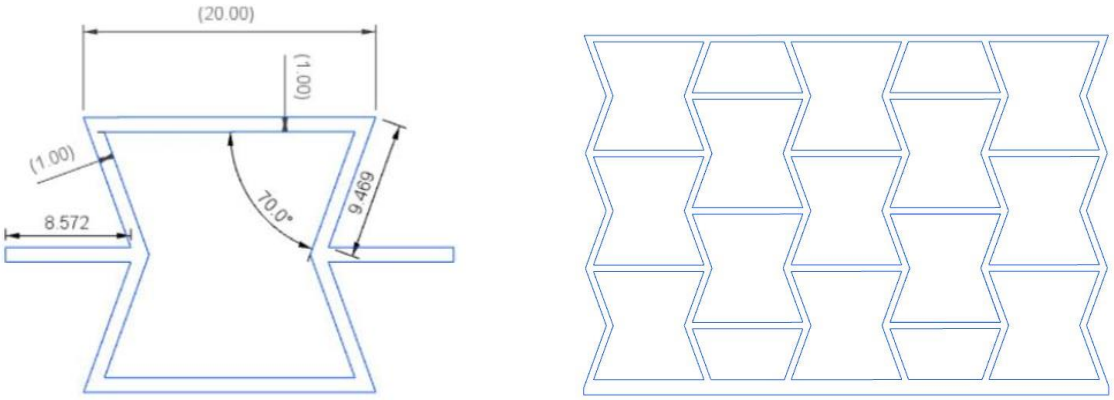

Figure 4. (a) Single unit cell and auxetic geometry, (b) lattice schematic.

(a)

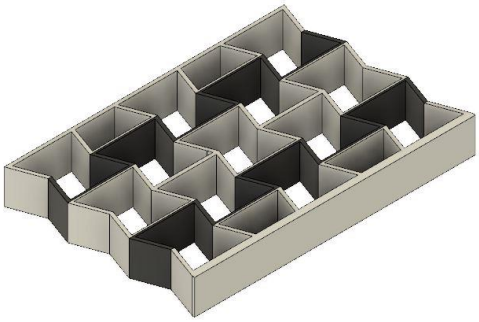

(b)

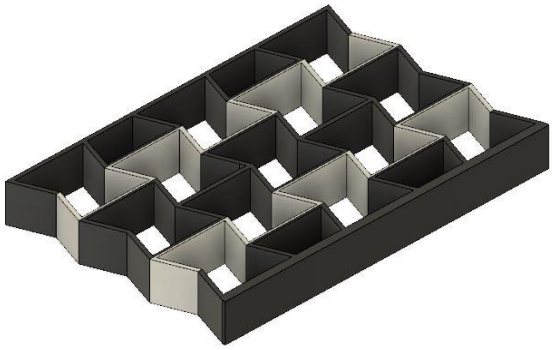

Figure 5. Dual-material auxetics: (a) SMP-FlexPro composed of pattern orientation SMP followed by FlexPro, (b) FlexPro-SMP composed of FlexPro followed by SMP (white and black colors correspond to SMP and FlexPro, respectively).

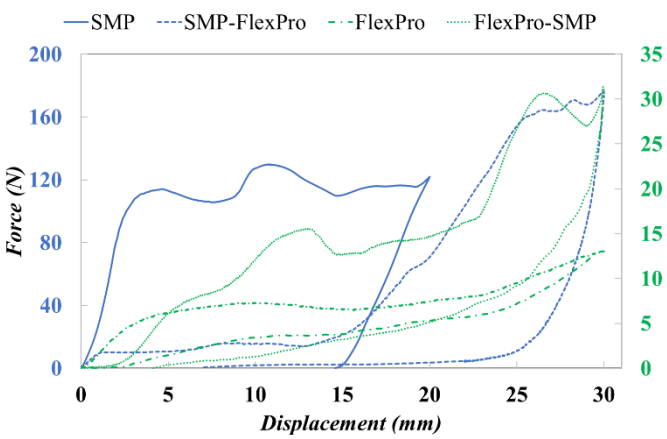

Figure 6. Experimental force-displacement response of four different meta-structures under a compressive loading-unloading cycle.

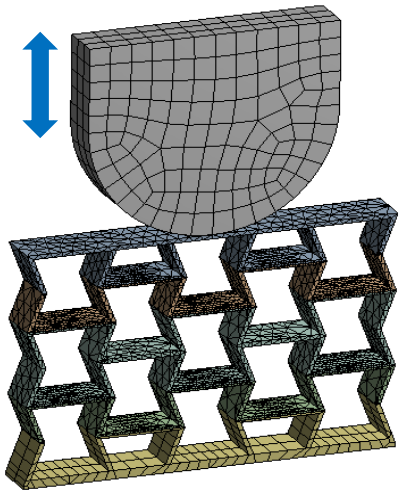

Figure 7. The auxetic meta-structure with generated mesh with span angle centre set to fine and transition state at slow.

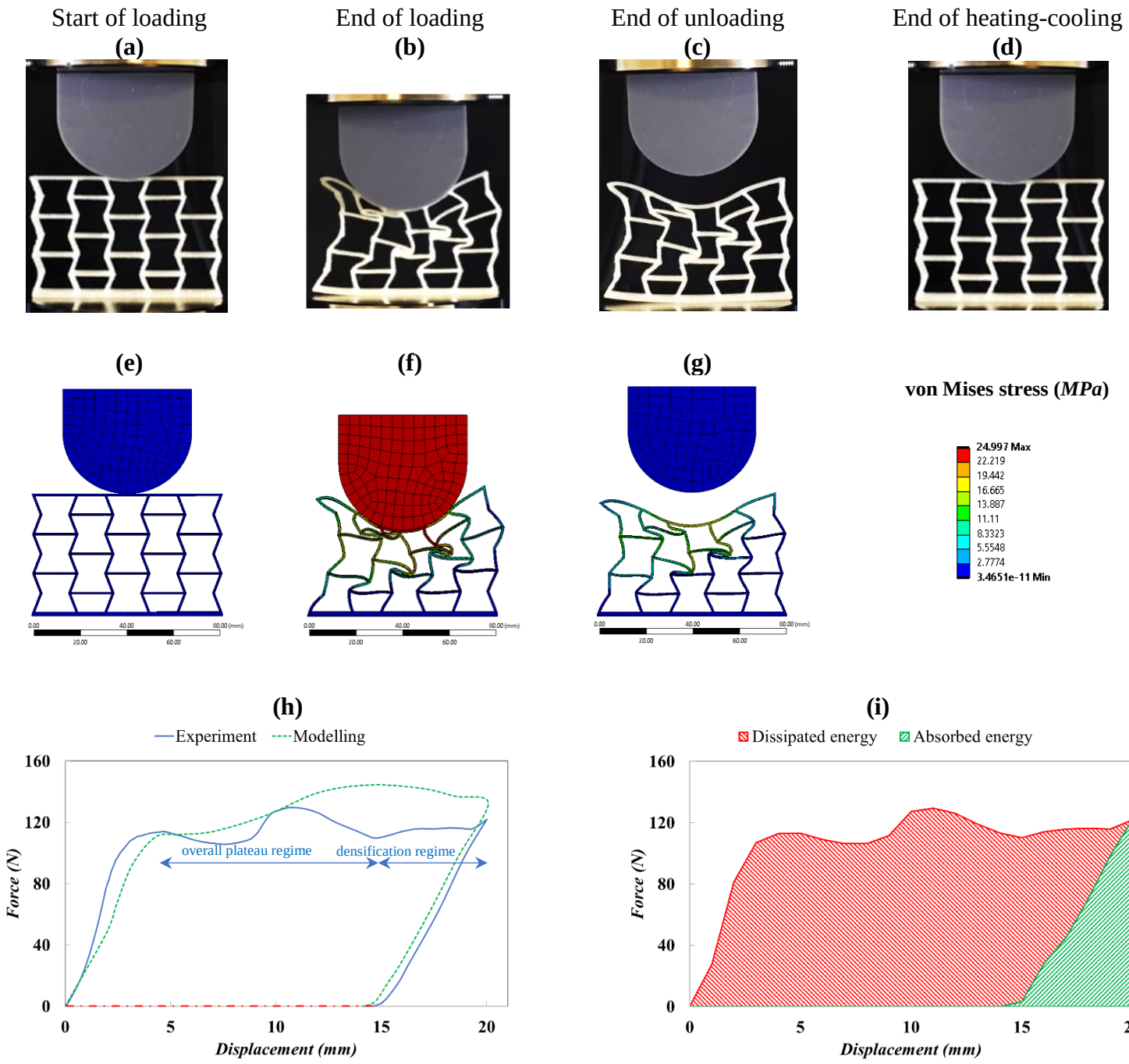

Figure 8. SMP meta-structure: (a)-(g) experimental and computational configuration, (h) force-displacement path for loading-unloading and thermal shape recovery (free strain recovery by thermal loading is represented by the red dash-dotted line), (i) dissipated and absorbed energies.

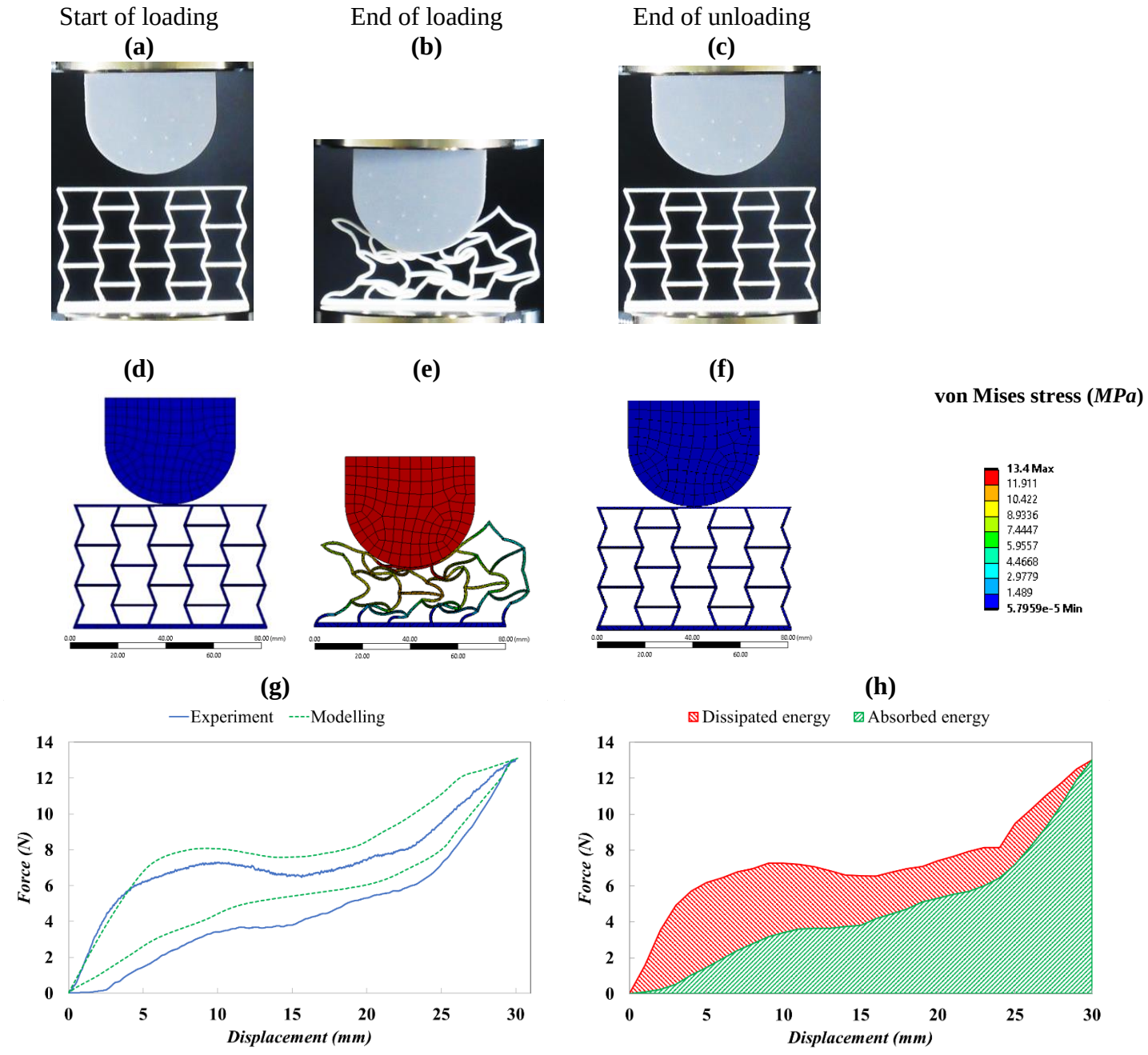

Figure 9. FlexPro meta-structure: (a)-(f) experimental and computational configuration, (g) force-displacement path for loading-unloading and thermal shape recovery, (h) dissipated and absorbed energies.

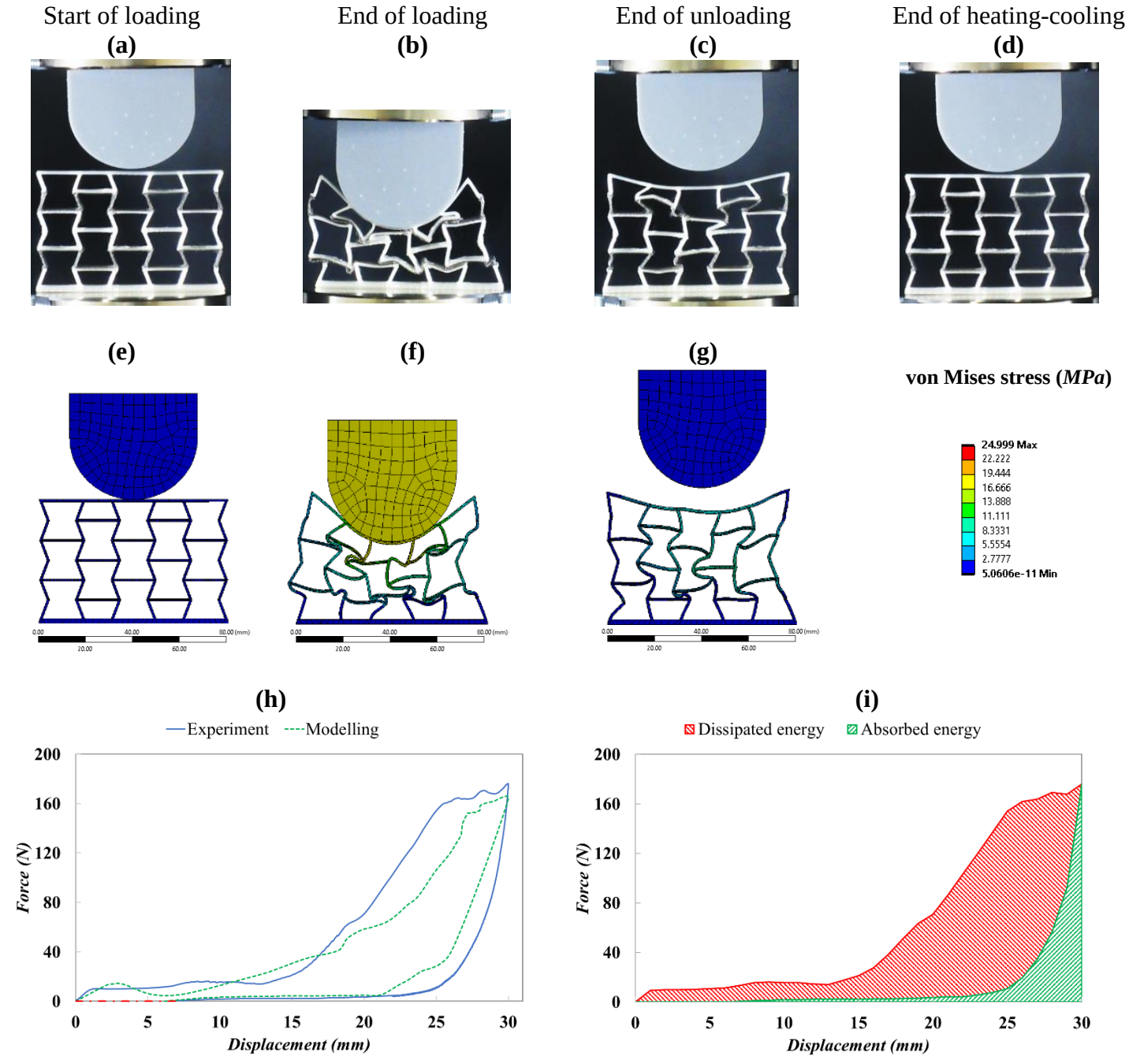

Figure 10. SMP-FlexPro meta-sandwich: (a)-(g) experimental and computational configuration, (h) force-displacement path for loading-unloading and thermal shape recovery (free strain recovery by thermal loading is represented by the red dash-dotted line), (i) dissipated and absorbed energies.

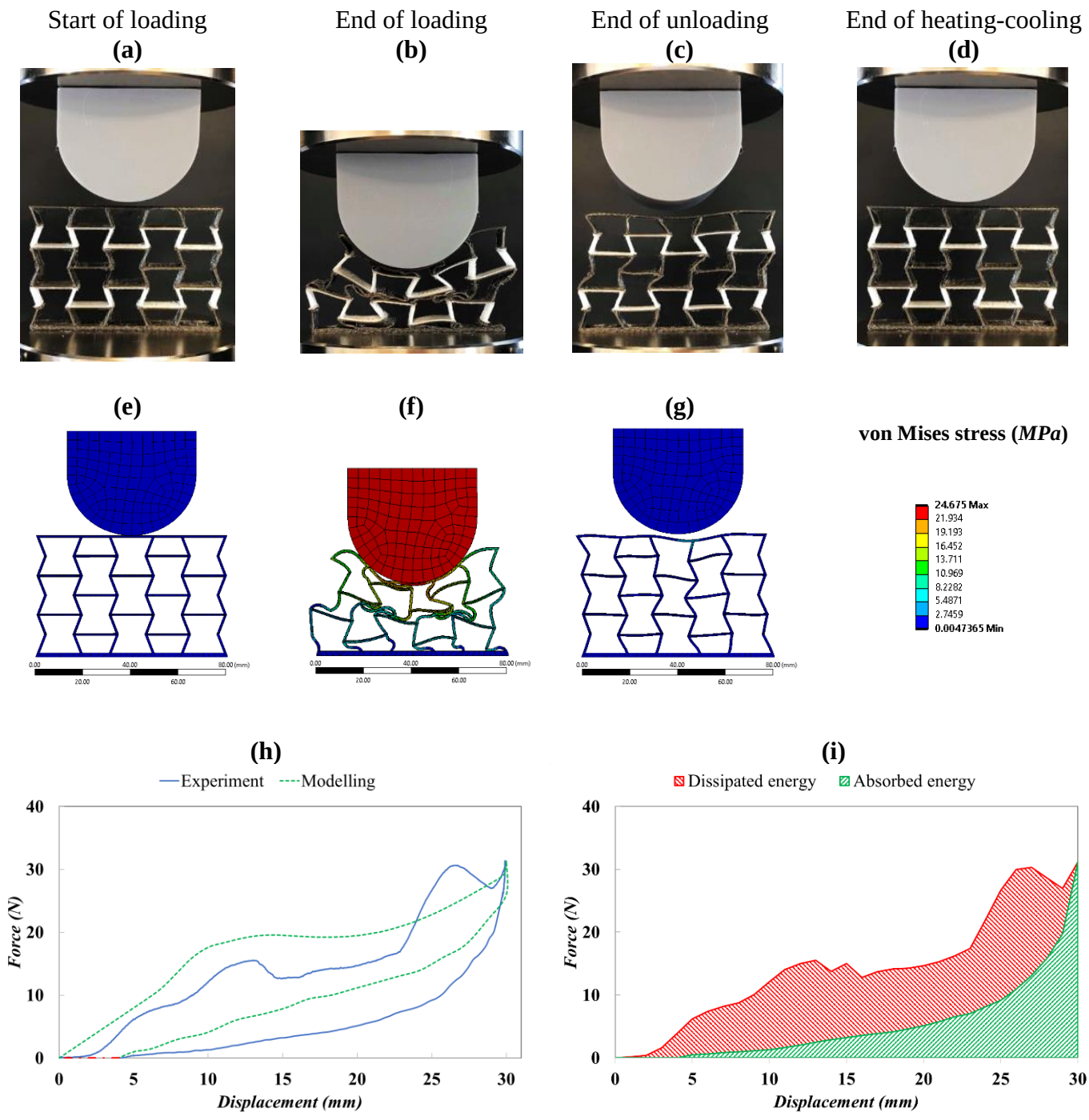

Figure 11. FlexPro-SMP meta-sandwich: (a)-(g) experimental and computational configuration, (h) force-displacement path for loading-unloading and thermal shape recovery (free strain recovery by thermal loading is represented by the red dash-dotted line), (i) dissipated and absorbed energies.